

# Facile Fabrication of Highly-Dispersed Nickel Nanoparticles with Largely Enhanced Electrocatalytic Activity

Xianggui Kong, Jingwen Zhao, Wenying Shi,\* Min Wei

State Key Laboratory of Chemical Resource Engineering, Beijing University of Chemical Technology, Beijing 100029, P. R. China

\*e-mail: shiwy@mail.buct.edu.cn

Received: March 15, 2013

Accepted: May 15, 2013

Published online: June 11, 2013

## Abstract

Supported nickel nanoparticles with high dispersion have been prepared by partial reduction of NiAl-layered double hydroxide (NiAl-LDH) precursors, which exhibit significant electrocatalytic behavior towards glucose. XRD and XPS results confirm that the nickel nanoparticles are successfully synthesized. TEM images reveal that the nickel nanoparticles are highly dispersed in the NiAl-LDH matrix with a size of  $6 \pm 0.3$  nm. The resulting nanocomposite modified electrode displays significant electrocatalytic performance to glucose with a broad linear response range ( $8.0 \times 10^{-5}$ – $2.0 \times 10^{-3}$  M), low detection limit (3.6  $\mu$ M), high sensitivity (339.2  $\mu$ A/mM), selectivity and excellent reproducibility as well as repeatability.

**Keywords:** Electrochemistry, High dispersion, Layered double hydroxides, Nickel

DOI: 10.1002/elan.201300127

Supporting Information for this article is available on the WWW under <http://dx.doi.org/10.1002/elan.201100127>.

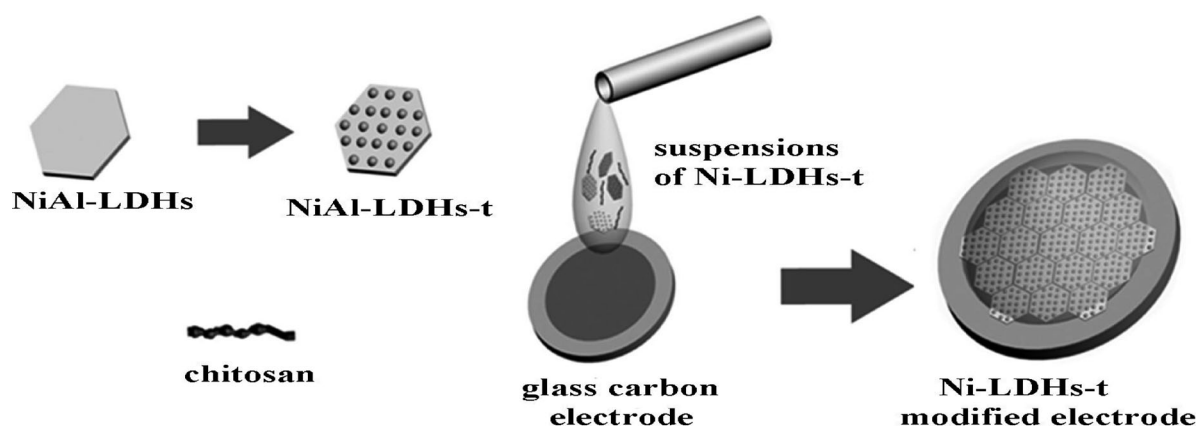
In recent years, nickel-based nanomaterials have attracted considerable attention in electrodes, magnetic storage devices and catalysis, owing to their excellent conductivity, strong magnetic property and excellent catalytic performance [1–3]. In the field of electrochemistry, highly dispersed nickel nanoparticles on a suitable support provide an efficient way of increasing electrochemical activity, because they can accommodate abundant superficial active sites facilitating mass/electron transfer in redox reaction [4]. Generally, surfactant-assisted approaches have been used to obtain the dispersed nickel nanoparticle [5,6]. However, some inherent demerits of the surfactant-assisted route, such as toxicity, relatively poor stability as well as a complicated fabrication process, limit the practical application of this method. Therefore, achieving supported nickel nanoparticles with high dispersion and enhanced activity is a challenging goal.

Layered double hydroxides (LDHs) are a class of naturally occurring and synthetic materials, which can be described as  $[M_{1-x}^{II}M_x^{III}(\text{OH})_2]^{z+}(A^{n-})_{z/n} \cdot y\text{H}_2\text{O}$  ( $M^{II}$  and  $M^{III}$  are divalent and trivalent metals respectively;  $A^{n-}$  is the interlayer anion compensating for the positive charge of the metal hydroxide layers), and have been widely used in the fields of catalysis, functional materials, sensors and drug delivery [7]. A unique structural characteristic of LDH materials is that the  $M^{II}$  and  $M^{III}$  cations are distributed in a highly-ordered manner in the hydroxide layers. Moreover, an in situ topotactic transformation of LDH materials to metal oxides or metal/metal oxide compo-

sites will occur upon heating in air or under reducing conditions, respectively [8]. This inspires us to fabricate the nickel nanoparticles with high-dispersion through reduction the NiAl-LDH layer, which exhibit the following advantages: firstly, the uniform dispersion of positive charge in the LDH nanosheets will result in a high dispersion of nickel nanoparticles and suppress their aggregation; secondly, the intrinsic topotactic phase transformation from the LDH matrix to supported Ni nanoparticles gives rise to a high stability for long-term employment. Furthermore, the size and dispersion degree of the nickel nanoparticles loaded on the matrix can be easily controlled.

In this work, highly dispersed Ni nanoparticles on the surface of NiAl-LDHs have been synthesized through partial reduction of NiAl-LDH precursors. The supported Ni nanoparticles on a LDH matrix (denoted as Ni-LDH-*t*, *t*=2, 4 and 6 h) modified electrode (Scheme 1) exhibits an excellent electrocatalytic performance to glucose. Therefore, this work demonstrates a successful paradigm for the fabrication of highly dispersed Ni nanoparticles, which can be potentially applied in the field of electrochemistry and electrochemical sensors.

Figure 1 A shows the XRD patterns of the as-synthesized samples. It was observed that a series of reflections indexed to a typical hydroxalcalite-like structure (JCPDS No. 48-0594) for the NiAl-LDHs (Figure 1 A, curve a). Compared with the NiAl-LDHs precursor, the Ni-LDHs-*t* samples display two new Bragg diffraction peaks at  $2\theta = 44.5^\circ$  and  $51.8^\circ$  (Figure 1 A, curves b, c and d), which can



Scheme 1. Schematic representation for the fabrication of Ni-LDH-*t* modified electrode.

be ascribed to the (111) and (200) reflections of metallic Ni with face-centered cubic (fcc) structure (JCPDS No. 04-0850). The results demonstrate reduction of the NiAl-LDH precursor gives rise to the formation of Ni nanoparticles embedded on the LDH matrix, which is proposed to be related to the topotactic transformation from Ni(OH)<sub>6</sub> octahedra in LDH layers to metallic Ni particles. NiAl-LDH nanoflakes serve as both Ni source and rigid template, which ensure a high dispersion of supported Ni nanoparticles as well as high stability. The conclusion was further supported by XPS results. Compared with NiAl-LDHs (Figure 1 B curve a), the XPS spectra of Ni-LDHs-*t* display signals attributed to metallic Ni 2P<sub>3/2</sub> (852.8 eV, Figure 1 B curves b, c and d) [9,10]. The ratio (Ni<sup>0</sup>/Ni<sup>0</sup> + Ni<sup>2+</sup>) of metallic Ni is 0.5%, 1.5% and 12% for the sample of Ni-LDHs-*t* (*t*=2, 4 and 6 h), respectively, indicating the increase of the amount of metallic Ni with increasing *t* (Figure S1). Furthermore, after partial reduction, the presence in a series of the reflections for the LDHs indicates that the existence of NiAl-LDH precursors (Figure 1 A curves b, c and d).

The growth process of Ni nanoparticles on the surface of NiAl-LDHs was monitored by TEM. Compared with the smooth surface of the NiAl-LDH layer (Figure 2 A), numerous nanoparticles emerged on the surface of the Ni-LDHs-*t* (*t*=2, 4 and 6 h, Figure 2 B, C and D), which can be attributed to the Ni nanoparticles based on the XRD and XPS results (Figure 1). The size of the Ni nanoparticles increased from 3 ± 0.5 nm to 10 ± 0.5 nm with increasing reduction time (from 2 to 6 h). The optimal quantity and high dispersion presents in the Ni-LDHs-4 sample with particle size of 6 ± 0.3 nm (Figure 2 C). The high magnification TEM of the Ni-LDHs-4 shows a single Ni nanoparticle with lattice interplanar spacing of 0.20 nm, corresponding to the (111) plane of a fcc Ni phase lattice fringes (inset in Figure 2 C). In contrast, an obvious aggregation of Ni nanoparticles was observed for the sample with reduction time of 6 h (Figure 2 D). Therefore, it is concluded that the reduction time plays a crucial role in determining the dispersion degree and the size of the Ni nanoparticles. Based on the results above, the Ni nanoparticles with high dispersion loaded on support can

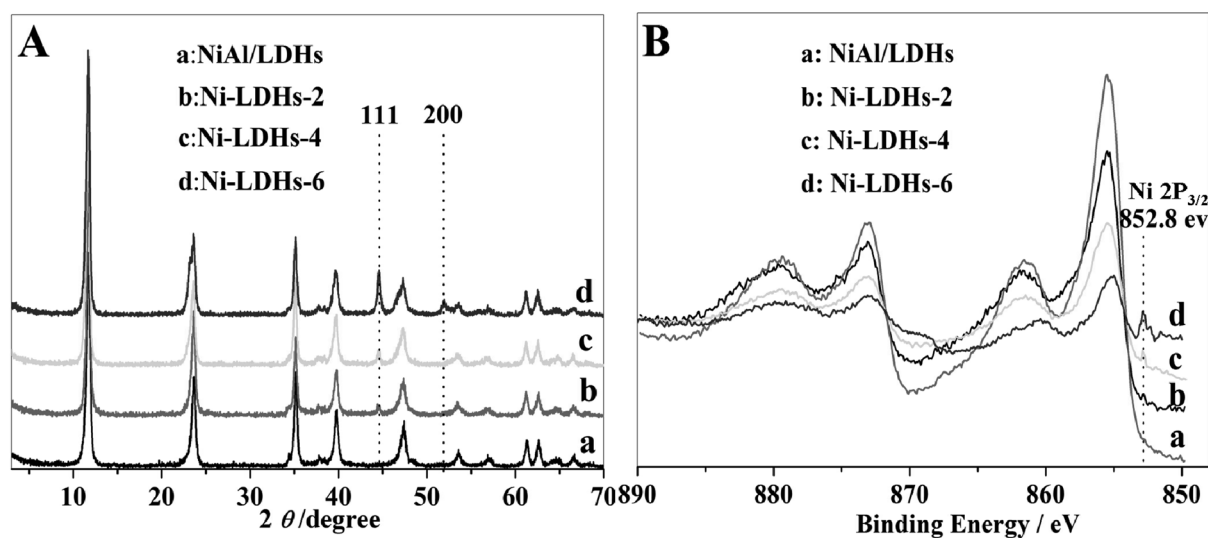


Fig. 1. (A) XRD patterns and (B) XPS spectra of the as-synthesized samples.

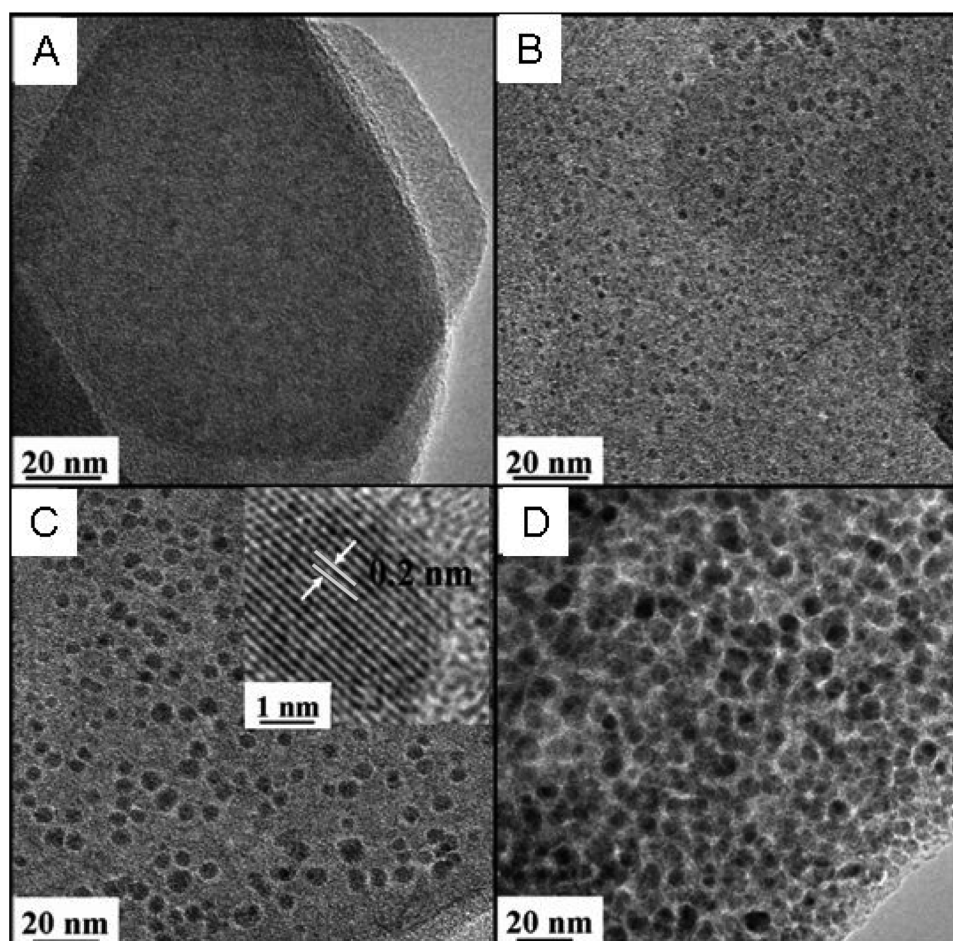
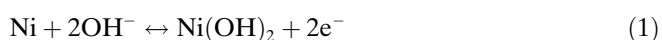


Fig. 2. TEM images of the (A) NiAl-LDHs and (B, C and D) Ni-LDHs- $t$  samples ( $t=2, 4$  and  $6$  h, respectively).

be facilely obtained by partial reduction of the NiAl-LDH precursor.

Figure 3A shows the cyclic voltammograms (CVs) of different electrodes in  $0.1$  M NaOH at a scan rate of  $0.1$  V s $^{-1}$ . Compared with the bare GCE and NiAl-LDH nanoplatelets modified electrode (Figure 3A, curve a and b), a pair of well-defined redox peaks with  $\Delta E_p = 72$  mV was observed ( $0.490/0.418$  V) for the Ni-LDHs-4 modified electrode (Figure 3A, curve c). The ratio between the anodic and cathodic peak current is  $\sim 1.05$ , indicating an excellent reversibility of the Ni-LDHs-4 modified electrode due to the high dispersion of Ni, which accelerate electron/mass transfer. This can be explained that high surface area due to high dispersion of Ni accommodates a large number of superficial active sites and much transportation pathways for the electron/mass in the redox process.

The redox transition can be described as follows [11]:



The electrochemical behavior of the Ni-LDHs- $t$  modified electrodes was also investigated (Figure 3B). It is

found that both the peak current and  $\Delta E_p$  of the Ni-LDHs- $t$  modified electrode increase with the enhancement of  $t$  value, indicating that the size and dispersion degree of the Ni nanoparticles play a crucial role in the electrochemical behavior. Taking into account both the  $\Delta E_p$  and peak current, the Ni-LDHs-4 modified electrode was chosen as the working electrode. Figure 3C displays the effect of scan rate on the electrochemical response of the Ni-LDHs-4 modified electrode, from which a linear relationship between the anodic (or cathodic) peak current and the potential sweep rate (from  $0.02$  to  $0.14$  V s $^{-1}$ ) was obtained, indicating a surface-controlled process. According to the Laviron theory and the plots of  $E_p$  vs.  $\log v$  (Figure 3D) [12], the electron transfer rate constant ( $K_s$ ) was calculated to be  $3.12$  s $^{-1}$ , larger than previously reported values for nickel modified electrode [13], displaying a fast electron transfer for the Ni-LDHs-4 sample.

Figure 4A displays the anodic peak current of the Ni-LDHs-4 modified electrode increasing significantly with the presence of glucose, demonstrating that the Ni-LDHs-4 has a strong electrocatalytic activity towards glucose. The positive shift of the anodic peak potential with increasing concentration of glucose attributes to the change in pH value due to the production of gluconolactone. Similar conclusions can be obtained from the study

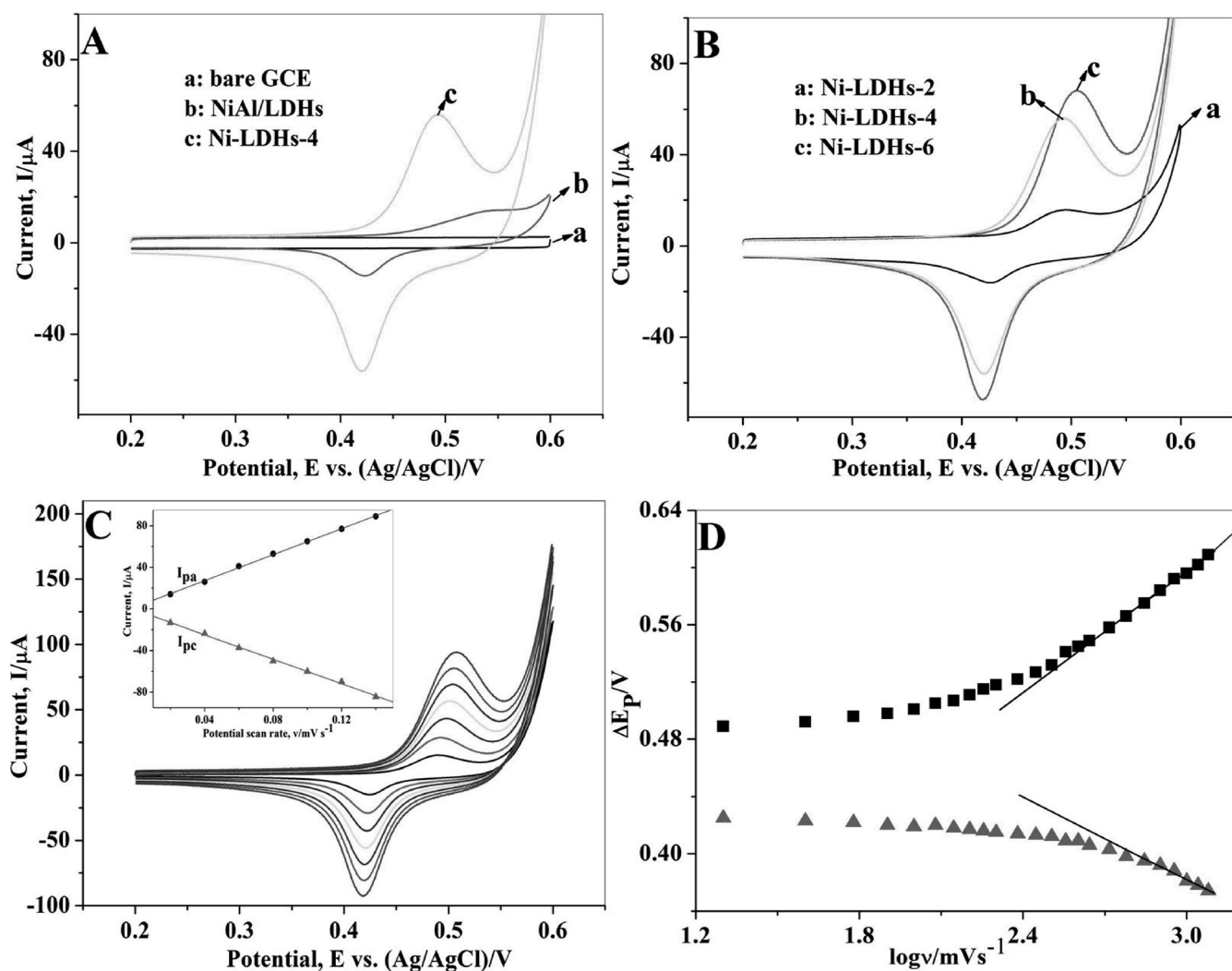


Fig. 3. (A) and (B) CVs obtained with different electrodes in 0.1 M NaOH; (C) CVs of the Ni-LDHs-4 modified electrode with different scan rate (inset: plots of peak current vs. scan rate); (D) plots of peak potential vs.  $\log v$  for the Ni-LDHs-4 modified electrode.

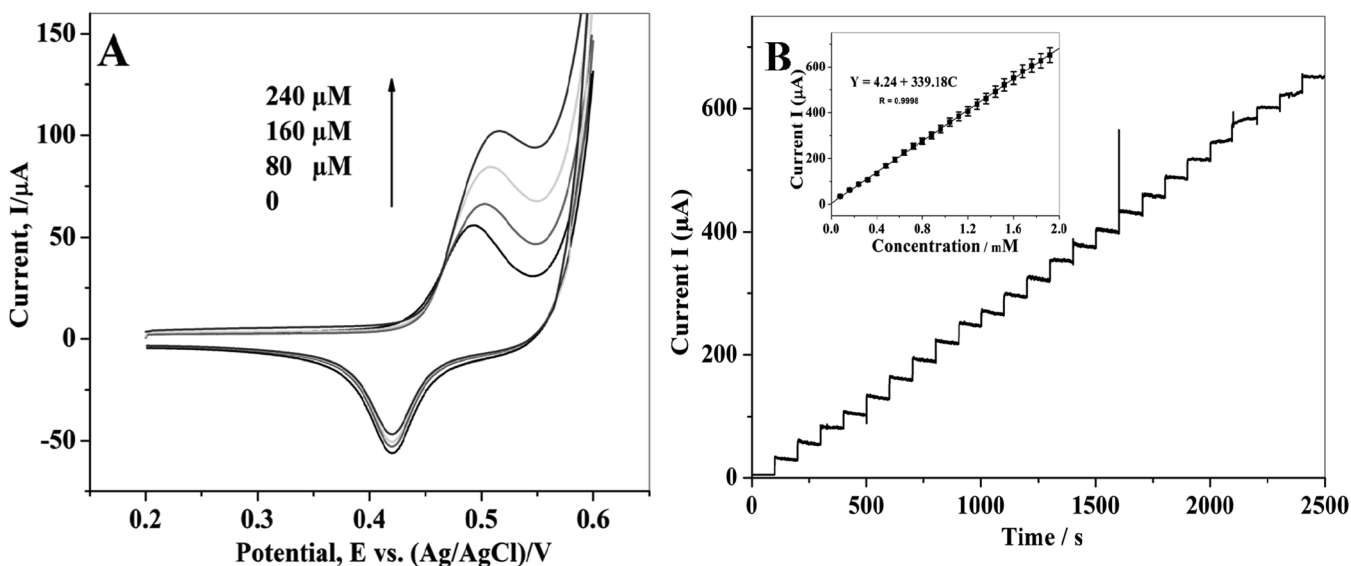


Fig. 4. (A) CVs of the Ni-LDHs-4 modified electrode with different glucose concentration in 0.1 M NaOH solution. (B) Typical amperometric response of the modified electrode to successive addition of 5  $\mu$ M glucose into 0.1 M NaOH solution ( $E=0.50$  V; Inset: Calibration curve of  $I-C$ ).

on the non-enzymatic detection of glucose based on acicular cobalt oxide nanorods. The amperometric response data show that the anodic peak current increases linearly with increasing glucose concentration from  $8 \times 10^{-5}$  to  $2 \times 10^{-3}$  M, with a linear regression equation of  $i$  ( $\mu\text{A}$ ) =  $4.24 + 339.18c$  (mM),  $r = 0.9991$  (Figure 4B), a detection limit of  $3.6 \mu\text{M}$ ,  $S/N = 3$  and sensitivity of  $339.2 \mu\text{A}/\text{mM}$ . This sensitivity is higher than previously reported for Ni-CME/GC ( $8.6 \mu\text{A}/\text{mM}$ ) measured in 1 M NaOH solution and nickel modified carbon ionic liquid electrodes measured in 0.5 M NaOH solution ( $202 \mu\text{A}/\text{mM}$ ) [14,15]. The interference tests show that the current produced by uric acid (UA), ascorbic acid (AA) and dopamine (DA) is only 2.1%, 1.4% and 2.9% compared with that of glucose (Figure S2), indicating a high selectivity of the Ni-LDHs-4 modified electrode towards glucose. Moreover, the Ni-LDHs-4 modified electrode exhibits good reproducibility ( $RSD > 1.5\%$  for 5 independently prepared electrodes). Repetition tests of one electrode shows that  $\sim 95.8\%$  of its initial current remains in consecutive 10 days measurement (Figure S3).

In summary, the supported Ni nanoparticles with high dispersion and enhanced electrochemical activity were synthesized via partial reduction of the NiAl-LDH precursor. The uniform dispersion of  $\text{Ni}^{2+}$  in the LDH nanoflake precursor induces a high dispersion of Ni nanoparticles and suppresses their aggregation in the in situ reduction process. The intrinsic topotactic phase transformation from the LDH matrix to supported Ni nanoparticles ensures a strong anchoring effect. Furthermore, the Ni-LDHs-4 modified electrode displays excellent electrocatalytic activity towards glucose. By virtue of the chemical versatility of LDH materials, it is expected that the approach in this work can be used to synthesize other supported transitional metal nanoparticles with enhanced behavior in electrocatalysis and electrochemical sensors.

### Experimental

**Reagents and Materials.** Glucose, UA, AA and DA were purchased from Alfa Aesar Chemical Co. Ltd. All other chemicals were of analytical grade and used without further purification. The solutions were prepared using water purified in a Milli-Q Millipore system ( $> 18.2 \text{ M}\Omega \text{ cm}$ ).

**Preparation of Ni-LDHs-*t* and its modified electrode.** The NiAl-LDHs were prepared according to the reported method [16]. 100 mL of a solution containing NiAl-LDHs (1 g),  $\text{NaHPO}_4$  (2 g) and NaOH (2 g) was hydrothermally treated in a Teflon-lined stainless steel autoclave at

$160^\circ\text{C}$  for different times ( $t$ ), then the precipitate was washed thoroughly, dried at  $60^\circ\text{C}$  to obtain the Ni-LDH- $t$  ( $t = 2, 4$  and  $6$  h). The  $10 \mu\text{L}$  suspensions of Ni-LDHs- $t$  ( $1 \text{ mg}/\text{mL}$ ) was treated ultrasonically, dropped on the surface of a glass carbon electrode ( $d = 3 \text{ mm}$ ) and dried under room temperature.

**Characterizations and electrochemical measurements.** Powder X-ray diffraction (XRD) patterns of the product were collected on a Rigaku XRD-6000 by use of  $\text{Cu-K}\alpha$  radiation at 40 kV, 30 mA. The morphology of the product was investigated using a JEOL JEM-2100 transmission electron microscope (TEM) with an accelerating voltage of 200 kV. A CHI 660B electrochemical workstation (Shanghai Chenhua Instrument Co., China) was utilized for electrochemical measurements.

### Acknowledgements

This project was supported by the *National Natural Science Foundation of China*, the *973 Program* (Grant No.: 2011CBA00504), the *Fundamental Research Funds for the Central Universities*.

### References

- [1] R. Jana, T. P. Pathak, M. S. Sigman, *Chem. Rev.* **2011**, *111*, 1417.
- [2] A. Babaei, M. Sohrabi, M. Afrasiabi, *Electroanalysis* **2012**, *24*, 2387.
- [3] G. W. Muna, A. Kaylor, B. Jaskowski, *Electroanalysis*, **2012**, *23*, 2915.
- [4] M. Zhang, Z. Yan, J. Xie, *Electrochim. Acta* **2012**, *77*, 237.
- [5] M. P. Zach, R. M. Penner, *Adv. Mater.* **2008**, *12*, 878.
- [6] C. Xu, Y. Hu, J. Rong, S. Jiang, Y. Liu, *Electrochem. Commun.* **2007**, *9*, 2009.
- [7] Q. Wang, D. O'Hare, *Chem. Rev.* **2012**, *112*, 4124.
- [8] M. Zhao, Q. Zhang, W. Zhang, J. Huang, Y. Zhang, D. Su, F. Wei, *J. Am. Chem. Soc.* **2010**, *132*, 14739.
- [9] K. S. Kim, N. Winograd, *Surf. Sci.* **1974**, *43*, 625.
- [10] J. T. Li, J. S'wiatowska, V. Maurice, A. Seyeux, L. Huang, S. G. Sun, P. Marcus, *J. Phys. Chem. C* **2011**, *115*, 7012.
- [11] M. Fleischmann, K. Karinek, D. Pletcher, *Electroanal. Chem.* **1971**, *31*, 39.
- [12] E. Laviron, *J. Electroanal. Chem.* **1979**, *101*, 19.
- [13] A. Salimi, E. Sharifi, A. Noorbakhsh, S. Soltanian, *Electrochem. Commun.* **2006**, *8*, 1499.
- [14] T. Watanabe, Y. Einaga, *Biosens. Bioelectron.* **2009**, *24*, 2684.
- [15] S. Kumar, P. Chen, S. Chien J. Zen, *Electroanalysis* **2005**, *17*, 210.
- [16] X. Kong, X. Rao, J. Han, M. Wei, X. Duan, *Biosens. Bioelectron.* **2010**, *26*, 549.